



Branch crack development from the flank of a fatigue crack propagating in mode II

Véronique Doquet, Joël Frelat

► To cite this version:

Véronique Doquet, Joël Frelat. Branch crack development from the flank of a fatigue crack propagating in mode II. *Fatigue and Fracture of Engineering Materials and Structures*, 2001, 24 (3), pp.207-214. 10.1046/j.1460-2695.2001.00384.x . hal-00111334

HAL Id: hal-00111334

<https://hal.science/hal-00111334>

Submitted on 18 Oct 2022

HAL is a multi-disciplinary open access archive for the deposit and dissemination of scientific research documents, whether they are published or not. The documents may come from teaching and research institutions in France or abroad, or from public or private research centers.

L'archive ouverte pluridisciplinaire **HAL**, est destinée au dépôt et à la diffusion de documents scientifiques de niveau recherche, publiés ou non, émanant des établissements d'enseignement et de recherche français ou étrangers, des laboratoires publics ou privés.



Distributed under a Creative Commons Attribution - NonCommercial 4.0 International License

Branch crack development from the flank of a fatigue crack propagating in mode II

V. DOQUET¹ and J. FRELAT²

¹Laboratoire de Mécanique des Solides. Ecole Polytechnique. UMR-CNRS 7649.91128 Palaiseau cedex France, ²Laboratoire de Modélisation en Mécanique, Université ParisVI. UMR-CNRS 7607. Tour 66, Case 162. 4 place Jussieu, 75252 Paris cedex 06, France

ABSTRACT The propagation of fatigue cracks in mode II often leads to the development of a branch starting from a crack flank, some distance behind the tip and not to the expected bifurcation at the crack tip. This type of branch is suggested to initiate by decohesion along a secondary slip plane and to grow in mode I due to the tensile component of the mode II stress field. Finite element calculations are performed to evaluate the stress intensity factors for the main crack and the branch as a function of the position of the latter. It is shown that the branch has a substantial shielding effect on the main crack and generates contact forces along its flanks. The simultaneous and competitive growth of the main crack and the branch in fatigue is simulated step by step using kinetic data for mode II and mode I obtained for a maraging steel.

Keywords branching; crack; fatigue; finite element; friction; mode II.

NOMENCLATURE

b = distance along the flanks from the main crack tip to the branch crack
 s = length of the branch crack behind the main crack tip
 K_{II} = stress intensity factor for the main crack
 k_I', k_{II}' = stress intensity factors for the branch crack behind the main crack tip
 k_I^* = stress intensity factor for a branch crack at the main crack tip.
 μ = friction coefficient

INTRODUCTION

Linear elastic fracture mechanics predicts that a crack loaded in plane shear will bifurcate in a direction for which the tangential stress is maximum (at an angle of -70.5° , according to Erdogan and Sih¹) or for which the mode I stress intensity factor is maximum ($k_I^* = 1.23K_{II}$) and the mode II stress intensity factor k_{II}^* is zero (at an angle of -77.3° , according to Amestoy *et al.*,² Bilby and Cardew³ as well as Wu⁴) not to mention other criteria based on energy density. As fatigue crack growth is a function of the stress intensity factor, Amestoy's criterion seems the most appropriate to analyse branching and will be used below.

Nevertheless, shear mode propagations have been observed over centimetric distances in fatigue, for sufficient levels of ΔK_{II} for which small scale yielding conditions however, still prevailed.⁵⁻⁷ As these fatigue cracks propagate under constant nominal loading ΔK_{II}^{nom} , the energy dissipated by the friction of their

flanks increases with a corresponding decrease in the effective stress intensity factor ΔK_{II}^{eff} . They decelerate, down to a given growth rate (corresponding to a transition threshold $\Delta K_{II,th}^{eff}$ estimated as $17 \text{ MPa}\sqrt{\text{m}}$ for a M250 maraging steel⁷) below which bifurcation occurs (In Ref. [7] it is suggested that this kind of bifurcation occurs when the mode I growth rate of the incipient branch crack at the main crack tip, submitted to $\Delta k_I^*(-77.3^\circ) = 1.23\Delta K_{II,th}^{eff}$ becomes higher than the mode II growth rate corresponding to $\Delta K_{II,th}^{eff}$).

However, in the aforementioned study on a maraging steel, mode II propagation was observed to end quite often by the development of a branch crack issued from a crack flank, some distance behind the main crack tip and not from the crack tip itself (Fig. 1). A recent paper by Murakami and Takahashi⁸ reports a similar observation on a medium carbon steel (see Fig. 4 of Ref [8]). Such a phenomenon is also reported for a 18-8 stainless steel and an LY12CZ aluminium alloy by Wang *et al.*⁹ (see Fig. 4 of Ref [9]). In the maraging steel, many



Fig. 1 Branching of a mode II crack from a crack flank in a maraging steel (the distance between engraved lines is 100 μm).

microcracks, more or less perpendicular to the main crack plane where observed along each of the crack flanks (Fig. 2). This is probably related to the activation of secondary slip systems at the crack tip (in addition to the coplanar primary slip system), followed by shear + tensile decohesion along the localized slip band. (Considering only the directions where the shear stress

$$\sigma_{r\theta} = \frac{K_{II}}{\sqrt{2\pi r}} \cos \frac{\theta}{2} \left(1 - 3 \sin^2 \frac{\theta}{2} \right)$$

is extremal, an inclination of $\pm 120^\circ$ of secondary slip planes would be predicted, but the activation of slip systems is also determined by local crystal orientations. As a result, most microbranches observed are more or less transverse, that is why this orientation is considered in the following). Once initiated and left behind by the advancing crack tip, those located along the flank where the stress

$$\sigma_{xx} = \frac{-K_{II}}{\sqrt{2\pi r}} \sin \frac{\theta}{2} \left(2 + \cos \frac{\theta}{2} \cos \frac{3\theta}{2} \right)$$

is tensile (i.e. for $\theta = -\pi$) will undergo mode I loading, with $K_{\min}/K_{\max} = 0$. After some propagation in the transverse direction due to this mode I loading, the branch

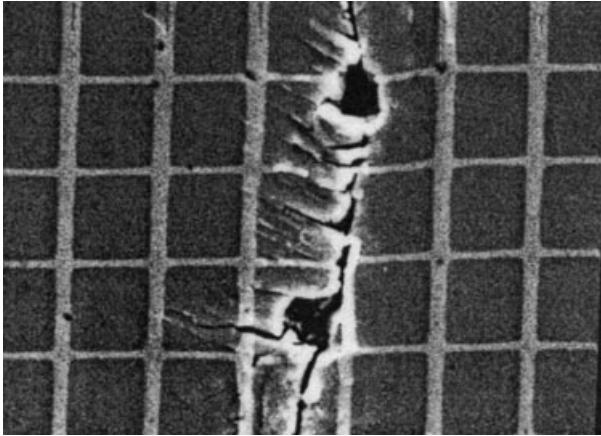


Fig. 2 Microcracks initiated along secondary slip bands on the flank of a mode II crack in a maraging steel. (pitch of the grids: 5 μm . Propagation downwards).

will finally bifurcate to grow at 45° to the main crack, along a principal plane. This final stage will not be considered here.

In a recent paper that prompted the present study, Kfoury¹⁰ suggested that this type of transverse branch crack sustains a higher stress intensity factor than the branch emanating from the crack tip itself with the inclination predicted by Erdogan and Sih¹ and might thus develop preferentially. Kfoury's calculations consider the singular stress field of the main crack, neglecting the redistribution of stresses due to the presence of the small branch. It will be shown below that this approximation is justified when the branch crack is far enough from the main crack tip.

The aim of this paper is to analyse, through finite element (FE) calculation, the influence of an incipient branch crack of length s , perpendicular to the main crack and located along the flank where $\sigma_{xx} > 0$, at a distance b behind its tip, on the stress field at the main crack tip [Fig. 3(a)] in order to explain, qualitatively, the unusual type of branching observed in mode II on maraging steel⁷ and some other alloys.^{8,9} Calculations are performed in elasticity (a correct analysis of the stress field behind the main crack tip in elasto-plasticity would require a node release procedure to simulate propagation, which is outside the scope of the present paper). The stress field at the branch tip is determined as a function of its position and the preference for bifurcation from the tip or for branching from a flank is discussed.

FINITE ELEMENT MODELLING OF INCIPIENT BRANCHING

As long as the branch is small, it generates only local stress redistributions and at some distance from the branch crack tip, the stress and strain fields are similar to those found without a branch. *In situ* experiments⁷ have shown that at the tip of the cracks grown in compact tension-shear (CTS) specimens loaded in shear, the relative crack flanks displacement were pure mode II. The aim here is not to represent the entire specimens but to analyse the stress field in a small area around the crack tip. Moreover, the initial growth of the branch is

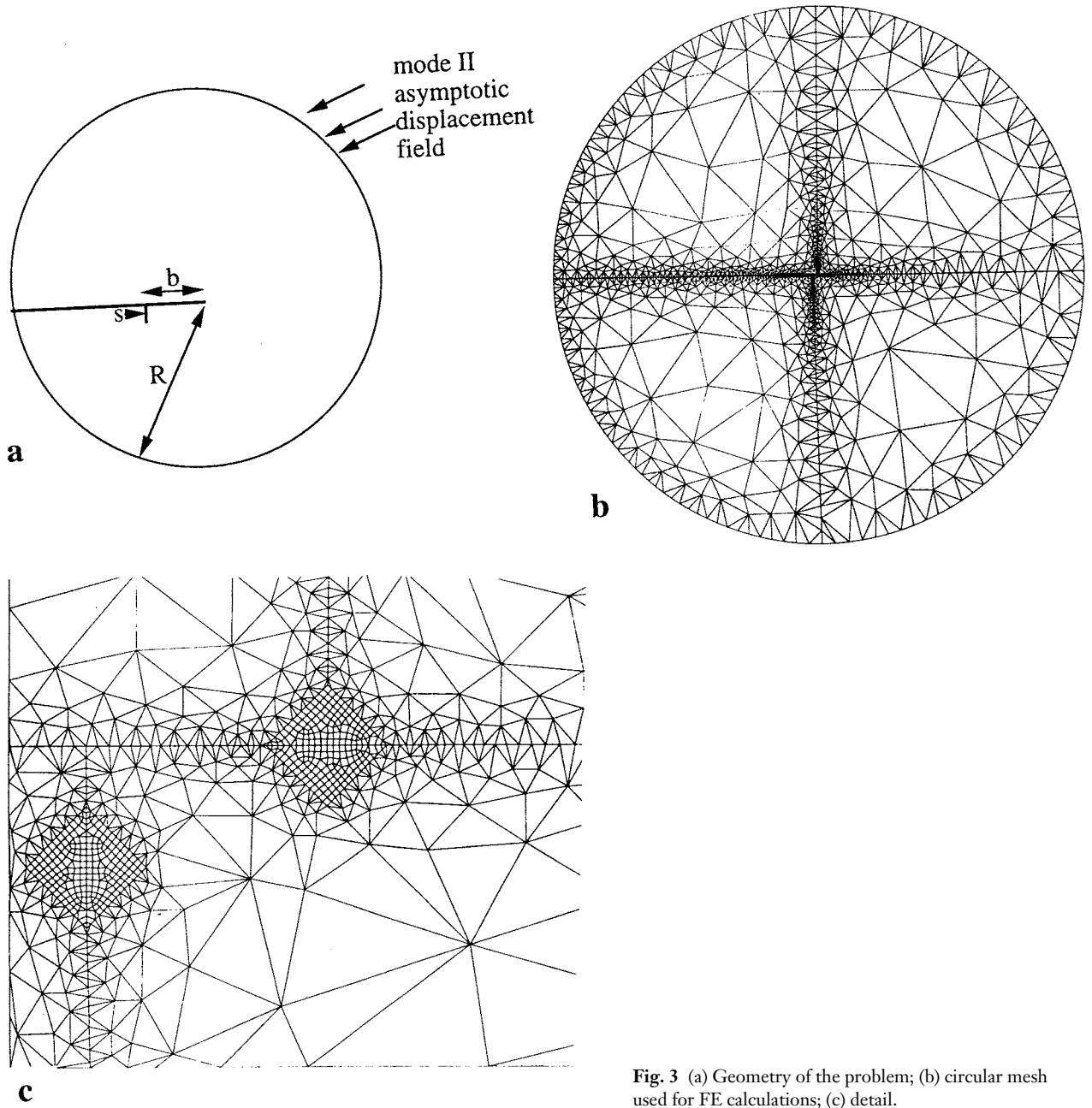


Fig. 3 (a) Geometry of the problem; (b) circular mesh used for FE calculations; (c) detail.

controlled only by the singular part of the stress field due to the main crack (i.e. the influence of far-field terms is negligible). For those reasons, a circular mesh containing the main crack and the branch was constructed with four nodes quadrilateral and three nodes triangular elements [Fig. 3(b),(c)]. The outer radius of the mesh, R is at least $20b$ and at least $100s$. The size of the elements around the branch crack tip is $s/10$ and around the main crack tip $s/20$. Since elastic behaviour is considered, results depend on the non-dimensional parameter b/s only. This parameter is varied from 0.25

to 20. The asymptotic displacement field corresponding to $K_{II} = 1 \text{ MPa}\sqrt{\text{m}}$ in plane strain is applied along the border of the mesh. (As the primary variables in the FE approximation of the variational formulation are displacements, fixed displacement boundary conditions are more accurate than fixed stresses. Furthermore this type of boundary conditions automatically eliminate rigid body motions).

Figure 4 shows how the plate deforms with these boundary conditions alone (with a large amplification). It can be seen on Fig. 4(b) that the branch crack opens

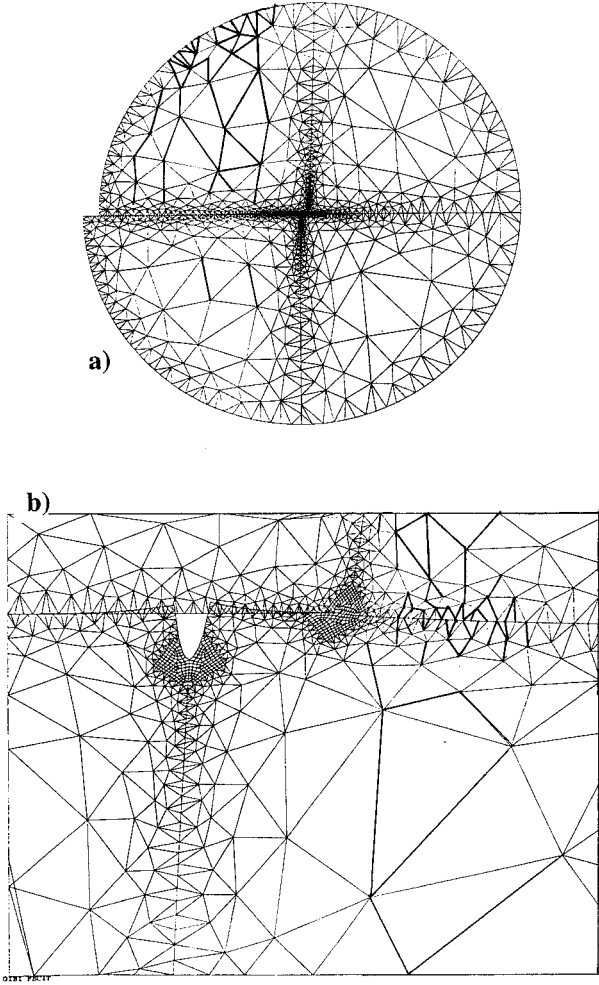


Fig. 4 (a) Deformed mesh (with a large amplification); (b) detail showing the interpenetration of the main crack flanks induced by the mode II component along the branch.

and that there is also a mode II component which induces some interpenetration of the main crack flanks. In the following, a condition of non-interpenetration was thus enforced. Two cases were considered: frictionless contact and Coulomb friction with a friction coefficient $\mu = 1$. The effective stress intensity factor of the main crack K_{II} , and those of the branch crack k'_I, k'_{II} were determined by a perturbation method¹¹ (virtual crack advance procedure named G-Théta in the CASTEM code) as a function of b/s . The number of layers of elements around the crack tip that were virtually moved to derive the energy release rate was varied between 1 and 10 and it was checked that the results did not depend on this number. The calculations were validated by the following test: the flanks of the branch were merged (thus keeping only the main straight crack) and the asymptotic displacement field corresponding to $K_{II} = 1 \text{ MPa}\sqrt{\text{m}}$ was imposed. The difference between

the prescribed unit value of K_{II} and the value computed by the G-Théta procedure was no more than $10^{-4}\%$ and K_I was zero with the same precision. When the branch is present, due to the perturbation it introduces, the accuracy of the computed values of the stress intensity factors is reduced to approximately 0.1%.

Frictionless contact

The evolution of the effective mode II stress intensity factor at the main crack tip as a function of the ratio b/s is plotted on Fig. 5. It can be seen that the branch has a strong shielding effect on the main crack. For $b/s = 0.25$, K_{II} is decreased by 50% compared to its apparent value which is recovered only when $b/s > 5$. This is the reason why the approximate calculation of k'_I as:

$$k'_I = \sigma_{xx} \sqrt{\pi s} = \frac{2K_{II} \sqrt{\pi s}}{\sqrt{2\pi b}} = K_{II} \sqrt{\frac{2s}{b}} \quad (1)$$

overestimates k'_I for small values of b/s if the apparent value of K_{II} (that is here $1 \text{ MPa}\sqrt{\text{m}}$) neglecting the shielding effect of the branch is used. This is illustrated on Fig. 6 where the values of k'_I issued from finite element calculations and from Eq. (1) are plotted as a function of b/s .

Knowing the effective value of K_{II} it is possible to evaluate the stress intensity factor $k^*_I = 1.23K_{II}$ of a potential branch emanating from the main crack tip with the angle of -77.3° predicted by Amestoy *et al.*² and to compare it with k'_I . This is done on Fig. 7. It appears that $k'_I > k^*_I$ if the branch located along the flank is close enough to the main crack tip ($b/s \leq 1.5$). Moreover, Fig. 8 shows that the branch is also submitted to a non-negligible mode II component, so that a comparison in terms of energy release rate is even more favourable to the branch located along the crack flank.

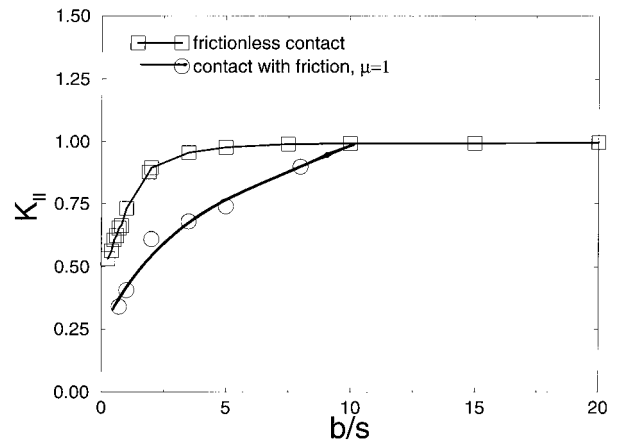


Fig. 5 Evolution of K_{II} at the main crack tip as a function of b/s .

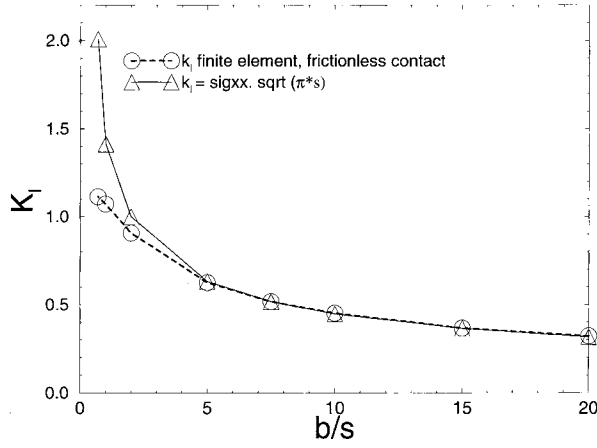


Fig. 6 Comparison of k_I obtained through finite element calculation (frictionless contact) with the approximate value obtained via Eq. (1).

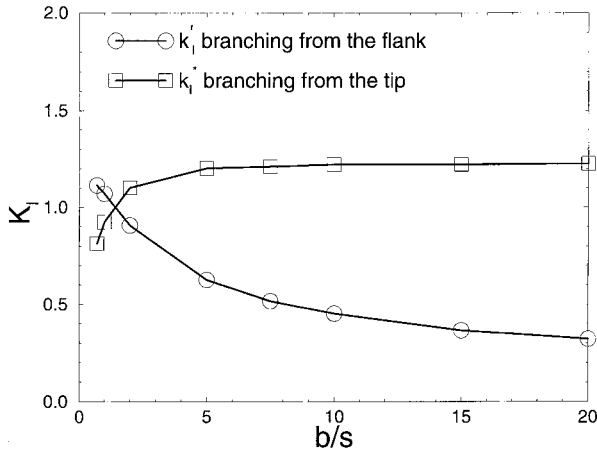


Fig. 7 Comparison of mode I stress intensity factors for the branch issued from the crack flank and a branch issued from the crack tip with an angle of -77.3° (frictionless contact).

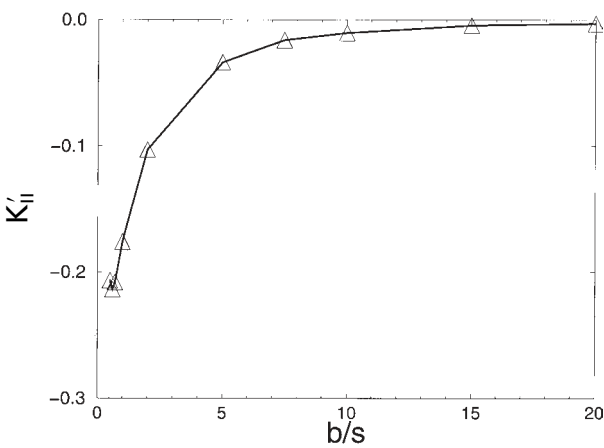


Fig. 8 Evolution of the mode II stress intensity factor for the branch as a function of b/s .

Coulomb friction

For that case, it was first checked that contact stresses are negligible in the immediate vicinity of the main crack tip, so that the perturbation method used to determine the stress intensity factors is still valid. In the range of low b/s values for which the branch is submitted to some mode II loading, the introduction of friction along the main crack flanks reduces the stress intensity factor K_{II} at its tip (Fig. 5). It also reduces k_I' and k_{II}' at the branch crack tip, but to a lesser extent, so that k_I'/k_I^* is increased and also $k_I' > k_I^*$ for a wider range of b/s ($b/s \leq 2$) (Fig. 9). For large values of b/s , the mode II component on the branch crack is zero, so that contact and friction do not affect the values of the stress intensity factors any more.

DISCUSSION

The results of finite element calculations with frictionless contact will now be used to simulate the competitive growth of the small branch and that of the main crack submitted to cyclic loading with constant ΔK_{II} and $K_{min}/K_{max} = 0$. The idea that the direction of fatigue crack growth under multiaxial loading is determined by a maximum velocity criterion, proposed by Hourlier *et al.*,¹² adopted by Tschegg and Stanzl,¹³ or Brown *et al.*¹⁴ to analyse branching from mode III to mode I, as well as by Pinna and Doquet⁷ for branching from mode II to mode I when branching occurs at the main crack tip is put in practice in these simulations where the fastest of the two cracks will unload the other one. The aim is just to derive a trend for the evolution of b/s when the branch is still small enough that its growth is governed by the singular part of the stress field at the main crack tip (it is clear that at a later stage, the branch

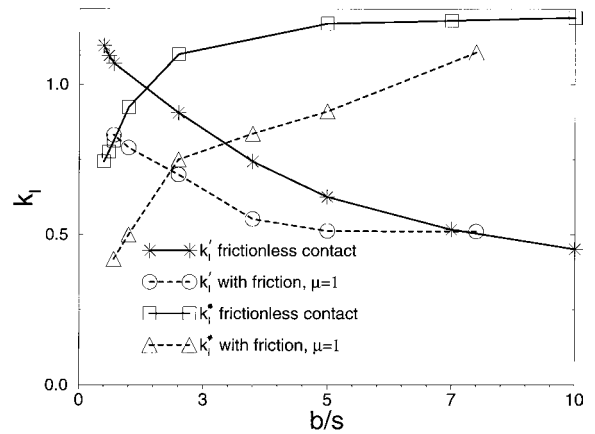


Fig. 9 Comparison of mode I stress intensity factors for the branch issued from the crack flank and a branch issued from the crack tip with an angle of -77.3° (contact with friction, $\mu = 1$).

will bifurcate to grow at 45° to the main crack, along a principal plane). The branch is considered to grow in mode I, neglecting the small mode II component.

Experimental data on mode I and mode II kinetics were obtained on a M250 maraging steel from tests performed on precracked CTS or tubular specimens with microgrids on their surface.^{7,15} Accurate measurements of the relative displacement profiles along the crack flanks were performed while the specimens were loaded inside a scanning electron microscope. An inverse analysis of the measured displacement profiles yielded the effective stress intensity factors, allowance made for friction forces due to asperities on the crack flanks. That way, the kinetic data plotted on Fig. 10 were obtained. The mode I kinetics can be described by: $da/dN = 10^{-7} \Delta K_I^2$ whereas for mode II for $\Delta K_{II} \geq 22 \text{ MPa}\sqrt{\text{m}}$, $da/dN = 4.1 \times 10^{-7} \Delta K_{II}^2$. Below this value, the curve for mode II, in spite of some scatter in the data, seems to bend and to cross the mode I kinetics around $18 \text{ MPa}\sqrt{\text{m}}$. This part of the curve has been described by a power law with a higher exponent. These data are used in the present study for a qualitative analysis of the unusual branching behind the main crack tip observed on this material.

An incremental calculation is performed: at each step, knowing b/s , the values of K_{II} and k'_I are deduced from previous finite element calculations and plugged in the mode II and mode I crack growth equations, respectively. b and s are then incremented and the loop starts again.

Two simulations have been performed with an initial branch length s of 0.02 mm and $b/s = 1$. In the first case ΔK_{II} was $40 \text{ MPa}\sqrt{\text{m}}$ and it can be seen on Fig. 11 that in spite of the shielding effect of the branch on the main

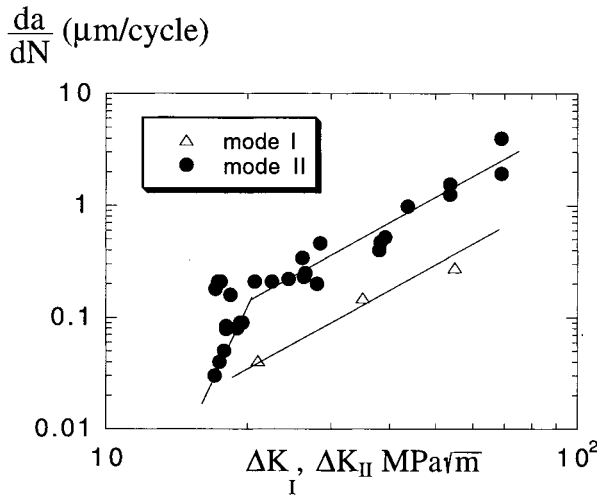


Fig. 10 Data on mode I and mode II fatigue crack growth kinetics in M250 maraging steel (from Refs [7] and [15]) used for the simulations.

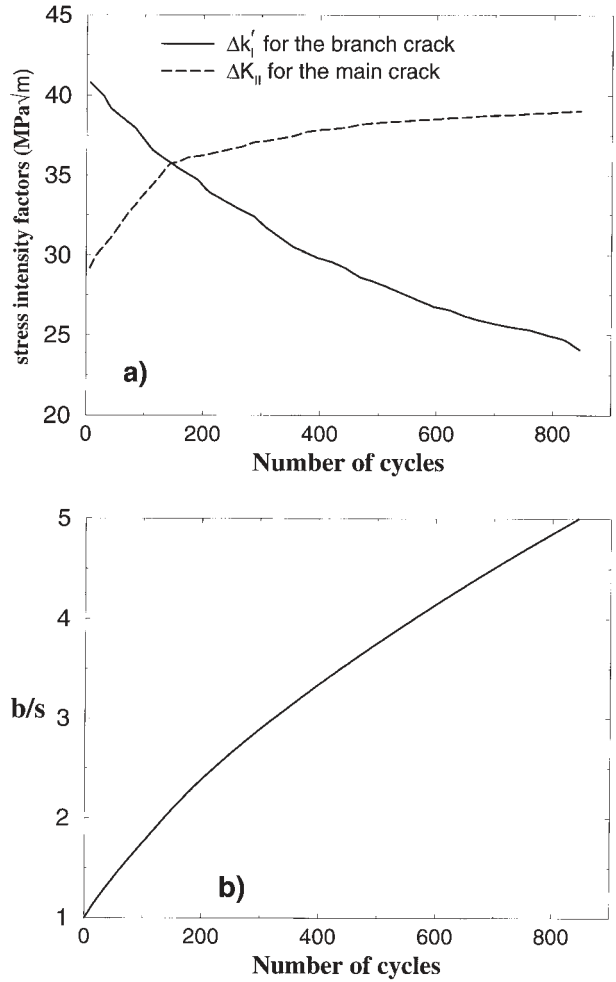


Fig. 11 Simulation of the simultaneous growth of the main crack and the branch for a test under $K_{II} = 40 \text{ MPa}\sqrt{\text{m}}$. (a) Evolution of the stress intensity factors; (b) evolution of b/s .

crack tip, the main crack propagates fast enough to leave the branch behind. The branch is thus unloaded progressively and the main crack recovers its normal stress intensity factor.

In the second simulation, ΔK_{II} was $26 \text{ MPa}\sqrt{\text{m}}$ which is closer to the bend in the mode II crack growth curve. Figure 12 shows that in that case, b/s decreases, which means that the branch crack grows faster than the main crack and tends to unload it.

This is qualitatively consistent with observations made by Murakami and Hamada¹⁶ who performed mode II propagation tests on a rail steel. They observed much 'partial local branching' on the fracture surfaces, inclined approximately 70° to the main crack (so that the mode I stress intensity factor undergone by these aborted branches when they are left behind the main crack tip is probably smaller than that calculated above for a transverse branch, but large similarities between both cases

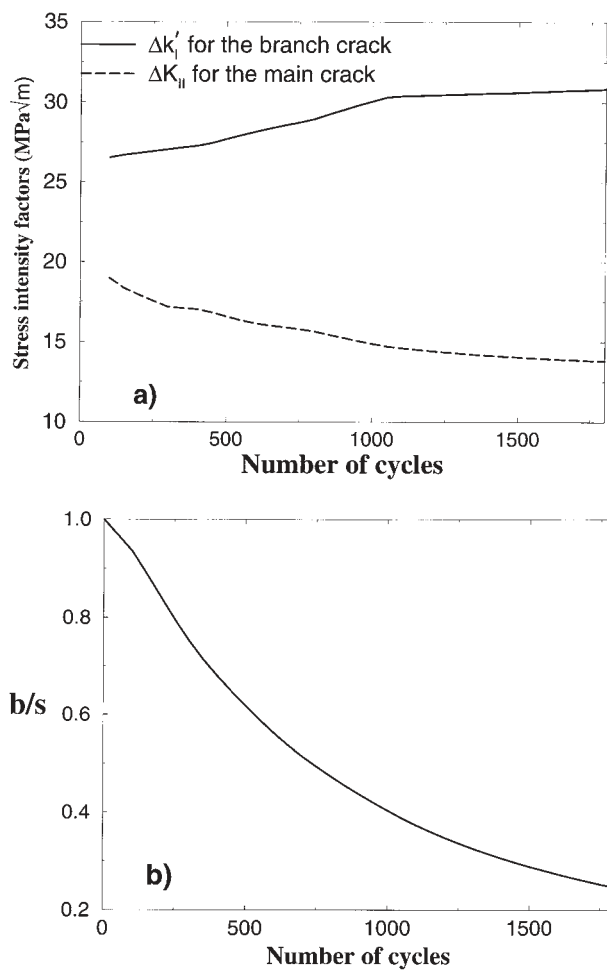


Fig. 12 Simulation of the simultaneous growth of the main crack and the branch for a test under $K_{II} = 26 \text{ MPa}\sqrt{\text{m}}$. (a) Evolution of the stress intensity factors; (b) evolution of b/s .

are believed to exist anyway). Murakami and Hamada report that the smaller the load (and thus the smaller ΔK_{II}), the more branching can be seen. Their test method correspond to a K -decreasing test which might explain many unsuccessful attempts for branching (ΔK_{II} too high, as in the first simulation of Fig. 11) resulting in many aborted small branch cracks on the fracture surface, before the final successful branch development can take place owing to a sufficiently low ΔK_{II} and thus sufficiently slow mode II crack growth.

They also report that when the specimen was lubricated, the branches were less numerous and their size was smaller. This is consistent with the present analysis based on a maximum velocity criterion. Lower friction forces between the asperities of the crack flanks should raise the effective mode II stress intensity factor (for a given nominal ΔK_{II}) and thus accelerate mode II crack growth, making competitive branching more difficult.

CONCLUSIONS

In a previous paper,⁷ the final bifurcation of mode II cracks grown under constant nominal ΔK_{II} in a maraging steel was analysed, using a maximum velocity criterion, for the case where branching takes place at the main crack tip. Experiments have shown that sometimes, the development of an initially transverse branch from the flank of a fatigue crack propagating in mode II may be preferred to bifurcation at the tip. The present FE analysis explains that this is due to the shielding effect of such a branch on the main crack and that it is more likely to occur when the mode II growth rate is small (due to a small effective ΔK_{II}) and when crack flank friction is high.

REFERENCES

- 1 Erdogan, F. and Sih, G. C. (1963) On the crack extension in plates under plane loading and transverse shear. *J. Basic Eng.* **85D**, 519–527.
- 2 Amestoy, M., Bui, H. D. and Dang Van, K. (1981) Analytic asymptotic solution of the kinked crack problem. *Adv. Fract. Res.* **1**, 107–113.
- 3 Bilby, B. A. and Cardew, G. E. (1975) The crack with a kinked tip. *Int. J. Fract.* **11**, 708–712.
- 4 Wu, C. H., (1978) Fracture under combined loads by maximum energy release rate extension. *J. Applied. Mech.* **45**, 553–558.
- 5 Otsuka, A., Mori, K., Oshima, T. and Tsuyama, S. (1981) Mode II fatigue crack growth in aluminium alloys and mild steel. In: *Advances in Fracture Research, Proceedings of the Fifth International Conference on Fracture, Volume 4*, (Edited by D. François). Pergamon Press, Oxford, UK, pp. 1851–1858.
- 6 Smith, M. C. and Smith, R. A. (1988) Toward an understanding of mode II fatigue crack growth. In: *Basic Questions in Fatigue, Volume 1*, ASTM-STP 924 (Edited by Fong, J. T. and Field, R. J.). American Society for Testing and Materials, Philadelphia, PA, USA, pp. 260–280.
- 7 Pinna, C. and Doquet, V. (1999) The preferred fatigue crack propagation mode in a M250 maraging steel loaded in shear. *Fatigue Fract. Engng. Mater. Struct.* **22**, 173–183.
- 8 Murakami, Y. and Takahashi, K. (1998) Torsional fatigue of a medium carbon steel containing an initial small surface crack introduced by tension-compression fatigue: crack branching, non-propagation and fatigue limit. *Fatigue Fract. Engng. Mater. Struct.* **21**, 1473–1484.
- 9 Wang, M. O., Hu, R. H., Qian, C. F. and Li, J. C. M. (1995) Fatigue crack growth under mode II loading. *Fatigue Fract. Engng. Mater. Struct.* **18**, 1443–1454.
- 10 Kfoury, A. P. (1999) A crack in a linear-elastic material under mode II loading, revisited. *Fatigue Fract. Engng. Mater. Struct.* **22**, 445–448.
- 11 Destuynder, Ph., Djaoua, M. and Lescure, S. (1983) Quelques remarques sur la mécanique de la rupture élastique. *J. Mécanique Théorique Appliquée* **2**, 113–135.
- 12 Hourlier, F., d'Hondt, H., Truchon, M. and Pineau, A. (1985) Fatigue crack path behavior under polymodal fatigue. In: *Multiaxial Fatigue*, ASTM-STP 853 (Edited by K. J. Miller and M. W. Brown). American Society for Testing and Materials, Philadelphia, PA, USA, pp. 228–248.

- 13 Tschegg, E. K. and Stanzl, S. E. (1988) The significance of sliding mode crack closure on mode III fatigue crack growth. In: *Basic Questions in Fatigue, Volume 1*, ASTM-STP 924, (Edited by Fong, J. T. and Field, R. J.). American Society for Testing and Materials, Philadelphia, PA, USA, pp. 214–32.
- 14 Brown, M. W., Hay, E. and Miller, K. J. (1985) Fatigue at notches subjected to reversed torsion and static axial loads. *Fatigue Fract. Engng. Mater. Struct.* **8**, 243–58.
- 15 Doquet, V., (2000) Effet de la fréquence de sollicitation et de l'environnement sur la propagation des fissures de fatigue en mode II, dans l'acier maraging. In: *19^{èmes} Journées de Printemps SF2M: Fatigue et environnement*, Paris, 24–25 Mai, (Edited by Hénatt, G., Baudry, G., Lieurade, H. P., Magnin, T. and Rémy, L.). SFZM, Paris, France, Paper 25.
- 16 Murakami, Y. and Hamada, S. (1997) A new method for the measurement of mode II fatigue threshold stress intensity factor range ΔK_{th} . *Fatigue Fract. Engng. Mater. Struct.* **20**, 863–70.